Atmos. Chem. Phys. Discuss., 11, 7155–7187, 2011
www.atmos-chem-phys-discuss.net/11/7155/2011/
doi:10.5194/acpd-11-7155-2011

Atmospheric Chemistry and Physics Discussions

Enhancement and depletion of lower/middle tropospheric ozone in Senegal during pre-monsoon and monsoon periods of summer 2008: observations and model results

G. S. Jenkins[1], S. Ndiaye[2], M. Gueye[2], R. Fitzhugh[3,*], J. W. Smith[1], and A. Kebe[4]

[1]Howard University Program in Atmospheric Science, Washington DC 20059, USA
[2]Lab for Atmospheric-Oceanic Physics-Simeon Fongang, Cheikh Anta Diop University, Dakar, Senegal
[3]Department of Atmospheric Ocean and Space Science, University of Michigan, Ann Arbor, Michigan, USA

[4]Senegal Meteorological Agency, Dakar, Senegal
[*]now at: ITT Corporation 1447 St. Paul Rochester, NY 14621, USA

Received: 24 November 2010 – Accepted: 27 February 2011 – Published: 2 March 2011

Correspondence to: G. S. Jenkins (gjenkins@howard.edu)

Published by Copernicus Publications on behalf of the European Geosciences Union.

ACPD
11, 7155–7187, 2011

Abstract

During the summer (8 June through 3 September) of 2008, nine ozonesondes are launched from Dakar, Senegal (14.75° N, 17.49° W) to investigate the impact of the Saharan Dust Layer (SAL) on ozone (O_3) concentrations in the lower troposphere. Results during June (pre-monsoon period) show a reduction in O_3, especially in the 850–700 hPa layer with SAL events. However, O_3 concentrations are increased in the 950–900 hPa layer where the peak of the inversion is found and presumably the highest dust concentrations. We use the WRF-CHEM model to explore the causes of elevated O_3 concentrations that appear to have a stratospheric contribution. During July and August (monsoon period), with the exception of one SAL outbreak, vertical profiles of O_3 are well mixed with concentrations not exceeding 55 ppb between the surface and 550 hPa. In the transition period between 26 June and 2 July lower tropospheric (925–600 hPa) O_3 concentrations are likely enhanced by enhanced biogenic NO_x emissions from the Saharan desert and Sahelian soils following several rain events on 28 June and 1 July.

1 Introduction

Understanding tropospheric ozone (O_3) variability in the tropics remains an active area of research with biomass burning, biogenic, anthropogenic and lightning being important sources of ozone production in the tropics and deposition and heterogeneous chemistry being important sink of O_3 in the tropics. A likely source of Northern Hemisphere summer season tropospheric O_3 variability is associated with Saharan dust events. Each year, between May and October, the Saharan Air Layer (SAL) (Prospero and Carlson, 1972; Dunion and Veldon, 2004) is a dominant feature influencing continental areas of West Africa and the Tropical Atlantic. The SAL is characterized by dry, (low relative humidity), stable air (an inversion capped above the marine boundary layer), a mid-level easterly jet and reduced visibilities from enhanced dust. Potential

ACPD
11, 7155–7187, 2011

sources of dust are found Mauritania, Mali and Algeria during June–July and August in association with the SAL (Middleton and Goudie, 2001).

A number of observational studies have shown reduced O_3 in the presence of Saharan Air Layer (SAL) outbreaks (De Reus et al., 2000; Bonasoni et al., 2004). The desert aerosols can reduce tropospheric O_3 concentrations at a single location in multiple ways: (a) dust aerosols may serve as deposition sites for O_3 while also reducing photolysis rates. (b) Heterogeneous chemistry on the aerosol site can reduce important precursors (OH, HO_2) associated with O_3 production. (c) The production of Nitric Acid (HNO_3), leading to particulate nitrate can act as a sink for NO_x and limit O_3 production (Zhang et al., 1994; Jacob, 2000; Bian and Zender, 2003; De Reus et al., 2000; Tang et al., 2003). Hence, the SAL acts as a potential sink for O_3, reducing its greenhouse forcing while also scattering solar radiation causing daytime cooling at the surface.

Recent observations of the SAL have examined its radiative impact (Myhre et al., 2003), chemical composition (Twohy et al., 2008) aerosol and water vapor structure (Ismail et al., 2010) and potential impact on African Easterly Waves (AEWs) and Tropical Cyclogenesis (Jenkins et al., 2008; Zipser et al., 2009). Here we report on the variability of lower/middle tropospheric O_3 (surface through 550 hPa) during the premonsoon and monsoon periods of 2008 at a location in the semi-arid Sahelian zone.

2 Observational data and model simulations

In preparation for examining ozonesonde launches during 2008, daily forecasts and ozonesonde preparation were conducted at Cheikh Anta Diop University–Dakar, Senegal. Vaisala ECC6AB ozonesondes were prepared 3–7 days in advance and launched in concert with RS92 radiosonde at 12:00 UTC during June, July and August of 2008. Table 1 shows the 9 ozonesonde launches from Dakar, Senegal (14.75° N, 17.49° W) during the period. Aerosol observations are derived from the Aerosol Optical Thickness (AOT) measurements from the Aerosol Robotic Network (AERONET) at Mbour,

ACPD
11, 7155–7187, 2011

Senegal (14.39° N, 16.59° W) and from the Space-borne Ozone Monitoring Instrument (OMI) Aerosol Index (AI) for the summer of 2008. The 1° × 1° Deep Blue product from the Moderate Resolution Imaging Spectrometer (MODIS) instrument aboard the AQUA satellite is used for AOT over land areas. Daily averages of AOT are constructed from the hourly AOT data from Mbour. Tropospheric Column Ozone (TCO) estimates for the summer of 2008 at 1° × 1.25° are also used (Ziemke et al., 2006).

The Weather and Research Forecasting with Chemistry (WRF-CHEM) model is used to simulate O_3 concentrations over West Africa during the summer of 2008 (Grell et al., 2005). The MOSAIC module in WRF-CHEM, which (Fast et al., 2005) includes gas phase chemistry, is used for simulating tropospheric O_3 over West Africa. The WRF-CHEM simulations use 30 km grid spacing, 27 vertical levels and the top of the model is 50 hPa. The biogenic sources of NO are computed (Guenther et al., 1994; Simpson et al., 1995) and the model is initialized from a uniform state with O_3 concentrations that increases with height to the stratosphere. NCEP final analyses at 6-h intervals provide meteorological boundary conditions to the WRF-CHEM. Here we define the pre-monsoon period as the month of June and the monsoon period from July through September.

3 Results

3.1 Pre-monsoon O_3 measurements

Figure 1a–d shows the satellite derived TCO values across West Africa and the Eastern Atlantic for June through September 2008. A north-south gradient of TCO values are found with higher TCO values are generally found over the Sahara relative to Sahelian and Guinean regions of West Africa. The TCO gradient is weakest and strongest during June and August respectively, when the lowest values are found at approximately 10° N over West Africa. TCO values of 37–40 DU are found over the desert regions during June through August, with the lowest values of 35–38 DU being found

ACPD
11, 7155–7187, 2011

over the Guinea region of West Africa. Figure 2a–c shows the OMI AI along with the AOT from Mbour, Senegal for the period of ozonesonde launches during 2008. There are a number of high AI/AOT days associated with SAL outbreaks during June and July and considerably fewer days in August. The numbers of days where AI was greater than 2.5 during June, July and August there were five, three and one respectively. The numbers of days where AOT values were greater than 0.6 during June, July and August there were seven, four and two, respectively. The OMI AI was positive correlated to the Mbour AOT values with correlation values of 0.82, 0.86 and 0.79 during June, July and August respectively. TRMM daily averaged rain amounts for a $5^{\circ} \times 5^{\circ}$ (11.5–16.5° N, 12.5–17.5° W) box over Senegal and Gambia shows very little precipitation until the end of June when wetter conditions begin and during July and August (Fig. 2d).

Figure 3a shows ozonesondes for the summer of 2008 with a range in O_3 concentrations from approximately 20–80 ppb between the surface and 450 hPa. Table 1 shows that highest column ozone in the 925–550 hPa layer is found on 12 June (20.5 DU) with 14.2 DU on 2 July. The lowest column ozone in the 925–550 hPa layer is found on 27 September (6.4 DU) followed by 8 June (6.6 DU). Figure 3b shows the two vertical profiles of O_3 between the end pre-monsoon period and the start of the monsoon season; a significant enhancement is found between the surface and 600 hPa. We discuss possible causes for elevated O_3 below.

There are three (3) ozonesonde launches, 8, 10, 15 June with OMI AI values >2 which are associated with SAL outbreak in Fig. 2. During the pre-monsoon period (Fig. 4a), O_3 concentrations are reduced on 8 and 10 June relative to the other profile, especially in the 850–600 hPa layer. These are also the two days with the lowest surface-550 hPa column ozone during the pre-monsoon period (Table 1). In the 950–900 hPa layer, just below the depleted layer there is also evidence of enhanced O_3 concentrations. Figure 4b shows low relative humidity (<20%) at approximately 950 hPa for 8, 10, 12 and 15 June, which begins to increase at pressure levels less than 700 hPa, except for 12 June where a RH values rapidly increase above 900 hPa. Figure 4c shows that a temperature inversion is present for all pre-monsoon ozone

ACPD
11, 7155–7187, 2011

profiles, but the very strongest temperature inversions are found for 8, 10 and 15 June. It is at the peak of temperature inversion that increases in O_3 concentrations are found (Fig. 4a). This is also the location where the dust concentrations tend to be the highest (Ismail et al., 2010).

Figure 5a–h shows OMI- AI with 925 hPa streamlines along with the Deep Blue AOT overlain by 700 hPa streamlines for comparison during the pre-monsoon period. Elevated aerosol loadings on 8, 10 and 15 June are associated with either northerly or northeasterly winds at 925 hPa (Fig. 5a, b, d). In contrast, winds with a southerly component are found on 12 June and 26 June (Fig. 5c, e); an African Easterly Wave (AEW) (Burpee et al., 1972) noted in the 700 hPa streamlines, exits the continent on 12 June and is associated elevated RH, cloudiness and precipitation in Dakar. Reduced O_3 between 850 and 600 hPa on 8, 10 June in concert with higher AI/AOT support the depletion through heterogeneous chemistry on the aerosol's surface.

3.2 Pre-Monsoon/Monsoon transition

Satellite and aircraft observations along with modeling studies have identified NO_x emissions from soil as a primary source of tropospheric NO_x during June, July and August in Sahelian and Saharan zones (Jeagle et al., 2004; Van der A et al., 2008; Williams et al., 2009; Delon et al., 2010). Pulses of biogenic NO_x emissions are released into the atmosphere from the soils at the end of the dry season with the first rains. During the 2006 African Monsoon Multidisciplinary Analyses (AMMA) campaign (Redelsperger et al., 2006), aircraft measurements flown over wet/dry soils during the AMMA field campaign show higher NO_x concentrations in the boundary layer over the recently wet soils (Stewart et al., 2008). O_3 concentrations were significantly higher over wet soils when compared to dry surfaces and low correlations with CO imply that NO_x production was not associated with anthropogenic or biomass burning sources (Stewart et al., 2008). A sharp gradient in O_3 concentrations were found implying produced locally O_3 estimated at 1 ppb h^{-1} from soil NO_x.

ACPD
11, 7155–7187, 2011

Figure 3b shows that O_3 concentrations between 950 and 600 hPa are considerably enhanced at the start of the monsoon period (2 July) when compared to the end of the pre-monsoon (26 June). O_3 concentrations are more than 10–20 ppb larger on 2 July when compared to 26 June. The enhancement of O_3 coincides with several rainfall events in Senegal that the vicinity of Dakar on 28, 30 June (Fig. 6a, b). TRMM daily rain estimates were highest on 1 July with daily amount approaching 80 mm in some areas to the east of Dakar (Fig. 6d). The rainfall was associated with the passage of an AEW on 1 July and a likely cause for O_3 enhancement between 26 June and 2 July by biogenic NO_x emissions from wet Sahelian soils.

3.3 Monsoon O_3 measurements and simulations

During the monsoon period, the vertical profiles of O_3 are nearly uniform on 2 July, 27 August and 3 September, except for 2 August when there is a SAL event impacting Senegal (Fig. 7a). The 2 August measurement shows the enhance/depletion pattern of O_3 concentrations in the vertical profile as in earlier SAL events with enhancement near the peak of the SAL temperature inversion and depletion immediately above this level. Figure 7b shows humid conditions over Senegal during July, August and September except for 2 August when a SAL event occurred over Senegal. The 2 August vertical profile of relative humidity shows values less than 10% in the 950–900 hPa layer. In contrast a very moist profile can be found on 27 August with RH values between 90 and 100% from 950 through 750 hPa. A large temperature inversion is found on 2 August in association with the SAL event with smaller temperature inversions found during the other three monsoon launches (Fig. 7c). Table 1 shows that during the monsoon period the lowest column O_3 is found on 27 August in association with the highest relative humidity during the entire period.

Figure 8a–h shows OMI- AI with 925 hPa streamlines along with the Deep Blue AOT overlain by 700 hPa streamlines for comparison during the monsoon period. During this period, only 2 August shows elevated AI and AOT in association with a thermal low that is found over Southern Mauritania (Fig. 8b). During the other three days, high AI

ACPD
11, 7155–7187, 2011

or AOT is found over higher latitudes where tobserved elevated thermal lows are found at latitudes higher than 20° N. Also evident at 700 hPa are strong AEWs, which have closed vortices on 2 July, 27 August and 3 September (Fig. 8a, c, d)

3.4 WRF-CHEM simulations of elevated O_3 concentrations on 12 June and reduced O_3 concentrations during the monsoon period with WRF-CHEM.

Table 1 shows that during the period of 10 June through 12 June, the column O_3 is increased by a factor of 2.77; between the SAL air mass and the passage of the AEW followed by a decreased by nearly a factor of 1.8 between 12 and 15 June. The elevated O_3 concentration on 12 June could be due to: (a) a stratospheric intrusion; (b) a biogenic pulse of NO_x from Sahelian soils enhancing O_3 or; (c) lightning-NO_x which enhances O_3 concentrations that is then transported to the lower/middle troposphere (Grant et al., 2008). The WRF-CHEM simulation suggests that a stratospheric intrusion is responsible for a large fraction of the increases in O_3 observed on 12 June. Figure 9a–d shows vertical profiles of O_3 at 14.5° N, 17.5° W near Dakar from four WRF-CHEM forecasts that have been initialized at 00:00 UTC, 1 June; 12:00 UTC, 4 June; 12:00 UTC, 5 June; 12:00 UTC, 6 June. Between the period of 8 June and 13 June higher concentrations of O_3 are found in the middle and upper troposphere; the higher O_3 corresponds to weak sinking motions over the period. During the early part of June rising motions are found at more equatorward areas of West Africa (land areas just north of the Gulf of Guinea) and sinking motions over the Sahel. WRF-CHEM forecasts that are initialized on 5 and 6 June show O_3 concentrations in the 90 to 120 ppb range on 11 and 12 June (Fig. 9c, d).

The elevated levels are consistent with the observations between 10 and 12 June where a large increase is found in the lower/middle troposphere (Fig. 4a). For example, O_3 values of 20 ppb are found near 600 hPa on 10 June but increase to nearly 65 ppb on 12 June. Figure 10 provides further support of a stratospheric intrusion when

ACPD
11, 7155–7187, 2011

comparing O_3 concentrations on 10, 12 June for 1000–150 hPa levels. On 12 June O_3 values greater than 400 ppb are found just below 200 hPa. The enhancement of O_3 relative to 10 June is found through the lower, middle and upper troposphere. Hence, O_3 elevated concentrations from the lower stratospheric is strongly supported by observations and WRF-CHEM results.

Table 1 shows low surface-550 hPa column O_3 under moist and low aerosol loading conditions. Relatively low concentrations of O_3 that are well mixed are found in the 27 August and 3 September measurements relative to earlier periods under humid conditions (Fig. 7a). There are several reasons that could lead to well mixed, reduced O_3 concentrations in the monsoon season: (a) increased O_3 and NO_x deposition; (b) the northward transport of O_3 poor air from areas to the south of the Sahel.

First, a reduction in O_3 concentrations during the monsoon period is expected because of increased deposition with the rapid growth of vegetation. After June, the northward movement of the monsoon and the accompanied southwest moist flow leads to increased instability and precipitation. The precipitation supplies an important source of moisture for vegetation growth of West Africa (Guinea northward to the Sahel). The expansion of vegetation leads to increased deposition and a north-south gradient in deposition rates and hence ozone in the lower troposphere. Measurements in Senegal during 2006 estimate a maximum deposition velocity of 1.5 cm s^{-1} with higher values noted during precipitation events (Grant et al., 2008). The removal of NO_x through dry/wet deposition would lead to reduced O_3 concentrations in lower latitudes relative to the drier semi-arid and arid regions in the Sahelian zone and Sahara desert (Delon et al., 2010).

Second, surges in the monsoon flow or the passage of AEWs should lead an overall poleward transport of lower O_3 concentration air, because of more vegetation and higher deposition rates. Conversely surges of dry air from desert regions should lead an equatorward transport of enriched O_3 concentrations to lower latitudes. The monthly averaged TCO values (Fig. 1) along with recent measurements during the African Monsoon Multidisciplinary Analyses (AMMA) field campaign support a north-south gradient

ACPD
11, 7155–7187, 2011

in the lower troposphere with lower O_3 concentrations found in equatorward latitudes of West Africa (Saunois et al., 2008).

Figure 11a shows the WRF-CHEM forecasted 925 hPa 12-h instantaneous O_3 concentrations averaged over the area of 14–16° and 18–16° W for June, July and August and early September. The highest O_3 concentrations are found during the month of June with significant reductions simulated during the months of July and August. Simulated O_3 concentrations of 10–20 ppb are common at 925 hPa during the monsoon period (Fig. 11a) relative to June. The lower simulated O_3 concentrations are found when the simulated relative humidity (RH) at 850 hPa values begins to increase (Fig. 11b). Elevated 850 hPa relative humidity can be used as a proxy of the southwesterly monsoon surge during July, August and September. The simulated increases in relative humidity are in agreement with satellite observed wetter conditions during July and August (Fig. 2d)

The poleward transport of O_3 poor air is the most likely reason for measured low O_3 concentrations in the lower troposphere measured at Dakar, Senegal for 27 August, and 3 September. After the 2 August SAL event, there are no additional SAL events in Senegal as noted in both the AI and AOT data. In each case, very moist conditions with flow coming from lower latitudes were found with the approach or recent passage of an AEW (Figs. 7b and 8c g, h) at 700 hPa. AEWs on 2 July and 27 August were associated with Tropical Cyclones Bertha and Ike, respectively.

4 Summary and conclusion

During the pre-monsoon period reductions of O_3 concentrations in the lower troposphere associated with SAL outbreaks. Figure 12a–d shows the vertical profiles of O_3 concentration, relative humidity and temperature in the 1000–750 hPa layer for the four SAL events that occurred during the summer of 2008. Similar vertical profiles of O_3 concentrations are found in three of the four ozonesondes: An increase in O_3 concentrations is found to overlap with a temperature inversion and very low relative humidity

ACPD
11, 7155–7187, 2011

(Fig. 12a, b, d). Note that there is a recovery in relative humidity on 2 August whereas relative humidity only slowly recovers in the other SAL events. In the 10 June and 2 August events, O_3 concentrations are reduced in the 900–750 hPa layer and generally lower than the surface values. The depletion is Fig. 12 is consistent with the earlier results of De Reus et al. (2000) and Bonasoni et al. (2004) with heterogeneous chemistry being a primary source of O_3 depletion (Zhang et al., 1994; Tang et al., 2004). Tang et al. (2004) show through modeling studies and aircraft observations that losses of O_3 and HNO_3 through direct interaction with dust were large during observed dust storms in the ACE-Asia field campaign.

Figure 13a depicts the changes in aerosol concentrations, relative humidity and O_3 concentrations based on the findings from this study. During a SAL event, a vertical profile of O_3 would show: Layer A – from the surface with slowly increasing O_3concentrations and low aerosol concentrations; Layer B – a 50–100 hPa layer with elevated O_3, high aerosols concentrations and a strong temperature inversion; Layer C – a 100–200 hPa layer with reduced O_3 concentrations and smaller sized aerosols. One might expect the largest losses of O_3 in layer B in association with heterogeneous reactions but the observations show that this isnot the case and hence there must be a source of O_3. The most likely source would be biogenic sources of NO_x from Saharan dust that act as a source of atmospheric O_3 in downstream regions. The exact mechanism for O_3 enrichment by Saharan dust remains uncertain.

A suggested mechanism for enhancing O_3 concentrations in this shallow layer may come from the activation of a biogenic NO_x pulse when encountering moist conditions (Fig. 13b). Nitrate formation on dust aerosols is an end-product after heterogeneous reactions between HNO_3 and dust aerosols. Gravitational settling of aerosols between 900–600 hPa that may have a significant amount of nitrate on aerosol surfaces through heterogeneous processes accumulate just above the inversion. At Dakar, very moist conditions (RH > 80%) are found from the surface to the 950 hPa just below the inversion associated with the SAL. Even though the inversion inhibits vertical motions, some mixing between the SAL layer and shallow moist layer below is possible.

ACPD
11, 7155–7187, 2011

Vlasenko et al. (2006) show in laboratory studies that nitrate-coated dust aerosols will increase their hygroscopicity in the presence of high relative humidity. Twohy et al. (2009) and Ismail et al. (2010) show that some SAL events have areas of enhanced moisture embedded within the SAL and that dust particles from the desert have hydroscopic properties and can serve as cloud condensation nuclei (CCN). A critical threshold of moisture on the surface of the aerosols could lead water stressed microbes to denitrify and release airborne biogenic NO_x leading to higher O_3 concentrations.

Other findings also include:

- Elevated O_3 concentrations on 12 June are likely caused by a stratospheric intrusion based on WRF-CHEM results and potentially enhanced NO_x emissions from dry Sahelian soils with the passage of an AEW. However, lightning-NO_x leading to O_3 enhancement followed by downward vertical transport by convective downdrafts cannot be ruled out as an additional source for 12 June (Jenkins et al., 2008b; Grant et al., 2008).

- During the transition between the pre-monsoon and monsoon periods (26 June and 2 July) a significant O_3 enhancement in the lower/middle troposphere are found after precipitation events in area surrounding Dakar on 28 June and 1 July 2008. We believe that pulses of biogenic NO_x emissions from dry Sahelian soils are the primary cause consistent with early studies (Stewart et al., 2008; Delon et al., 2008, 2010).

- Low O_3 concentrations are found in the 1000–550 hPa layers during the monsoon period (27 August and 3 September) and likely linked to dry deposition of O_3 and dry/wet deposition NO_x and HNO_3 during the monsoon period (Grant et al., 2008; Delon et al., 2010).

Additional chemical, radiative and aerosol measurements along with chemical modeling on a regional basis in West Africa will provide additional insights into the processes that control O_3 concentrations in the lower troposphere.

ACPD
11, 7155–7187, 2011

Acknowledgements. This work was supported by ATM-0621529. We thank all of the Met operators for their help in this project. We thank Didlier Tanre for their efforts in establishing and maintaining the Mbour, Senegal site.

References

Bian, H. and Zender C. S.: Mineral dust and global tropospheric chemistry: Relative roles of photolysis and heterogeneous uptake, J. Geophys. Res., 108, 4672, doi:10.1029/2002JD003143, 2003.

Bonasoni, P., Cristofanelli, P., Calzolari, F., Bonafè, U., Evangelisti, F., Stohl, A., Zauli Sajani, S., van Dingenen, R., Colombo, T., and Balkanski, Y.: Aerosol-ozone correlations during dust transport episodes, Atmos. Chem. Phys., 4, 1201–1215, doi:10.5194/acp-4-1201-2004, 2004.

Camara, M., Jenkins, G., and Konare, A.: Impacts of dust on West African climate during 2005 and 2006, Atmos. Chem. Phys. Discuss., 10, 3053–3086, doi:10.5194/acpd-10-3053-2010, 2010.

Carlson, T. and Prospero, J. M.: The Large-Scale Movement of Saharan Air Outbreaks over the Northern Equatorial Atlantic, J. Appl. Meteorol., 11, 283–297, 1972.

De Reus, M., Dentener, F., Thomas, A., Borrmann, S., Ström, J., and Lelieveld, J.: Airborne observations of dust aerosols over the North Atlantic during ACE2: Indications for heterogeneous ozone destruction, J. Geophys. Res., 105, 15263–15275, 2000.

Delon, C., Reeves, C. E., Stewart, D. J., Sera, D., Dupont, R., Mari, C., Chaboureau, J.-P., and Tulet, P.: Biogenic nitrogen oxide emissions from soils impact on NO_x and ozone over West Africa during AMMA (African Monsoon Multidisciplinary Experiment): modelling study, Atmos. Chem. Phys., 8, 2351–2363, doi:10.5194/acp-8-2351-2008, 2008.

Delon, C., Galy-Lacaux, C., Boone, A., Liousse, C., Sera, D., Adon, M., Diop, B., Akpo, A., Lavenu, F., Mougin, E., and Timouk, F.: Atmospheric nitrogen budget in Sahelian dry savannas, Atmos. Chem. Phys., 10, 2691–2708, doi:10.5194/acp-10-2691-2010, 2010.

Dunion, J. P. and Velden C. S.: The impact of the Saharan air layer on Atlantic tropical cyclone activity, B. Am. Meteorol. Soc., 85, 353–365, doi:10.1175/BAMS-85-3-353, 2004.

Fast, J. D., Gustafson, W. I., Easter, R. C., Zaveri, R. A., Barnard, J. C., Chapman, E. G, Grell, G. A., and Peckham, S. E.: Evolution of ozone, particulates, and aerosol direct radiative

ACPD

11, 7155–7187, 2011

forcing in the vicinity of Houston using a fully coupled meteorology-chemistry-aerosol model, J. Geophys. Res., 111, D21305, doi:10.1029/2005JD006721, 2006.
Grant, D. D., Fuentes, J. D., DeLonge, M. S. , Chan, S. , Joseph, E. , Kucera, P. , Ndiaye, S. A., and Gaye, A. T.: Ozone Transport by Mesoscale Convective Systems in Western Senegal, Atmos. Environ., 42, 7104–7114, 2008.
Grell, G. A., Peckham, S. E., Schmitz, R., McKeen, S. A., Frost, G., Skamarock, W. C., and Eder B.: Fully coupled "online" chemistry within the WRF model, Atmos. Environ., 39, 6957–6975, 2005.
Guenther, A., Zimmerman, P., and Wildermuth, M.: Natural volatile organic compound emission rate estimates for US woodland landscapes, Atmos. Environ., 28, 1197–1210, 1994.
Ismail, S., Ferrare, R. A., Browell, E. V., Chen, G., Anderson, B., Kooi, S. A., Notari, A., Butler, C. F., Burton, S., Fenn, M., Dunion, J. P., Heymsfield, G., Krishnamurti, T. N., and Mrinal, K.: LASE Measurements of Water Vapor, Aerosols and Cloud Distributions in Saharan Air Layers and Tropical Disturbances, J. Atmos. Sci., 67, 1026–1047, 2010.
Jacob, D. J.: Heterogeneous chemistry and tropospheric ozone, Atmos. Environ., 24, 2131–2159, 2000.
Jaegle, L., Martin, R. V., Chance, K., Steinberger, L., Kurosu ,T. P., Jacob, D. J., Modi, A. I., Yoboue, V., Sigha-Nkamdiou, L., and Galy-Lacaux, C.: Satellite mapping of rain-induced nitric oxide emissions from soils, J. Geophys. Res., 109, D21310, doi:10.1029/2004JD004787, 2004.
Jenkins, G. S., Pratt, A. S., and Heymsfield, A.: Possible linkages between Saharan dust and Tropical Cyclone Rain Band Invigoration in Eastern Atlantic during NAMMA-06, Geophys. Res. Lett., L08815, doi:10.1029/2008GL034072, 2008.
Jenkins, G. S., Camara, M., and Ndiaye, S.: Observational Evidence of enhanced middle/upper tropospheric ozone via convective processes over the Equatorial Tropical Atlantic during the summer of 2006, Geophys. Res. Lett., 35, L12806, doi:10.1029/2008GL033954, 2008b.
Kalnay, E., Kanamitsu, M., Kistler, R., Collins, W., Deaven, D., Gandin, L., Iredell, M., Saha, S. White, G., Woollen, J., Zhu, Y., Leetmaa, A., Reynolds, R., Chelliah, M., Ebisuzaki, W., Higgins, W., Janowiak, J., Mo, K. C., Ropelewski, C., Wang, J., Jenne, R., and Joseph, D.: The NCEP/NCAR 40 year reanalysis project, B. Am. Meteorol. Soc., 77, 437–471, 1996.
Middleton, N. J. and Goudie, A. S.: Saharan dust: Sources and trajectories, T. I., Brit. Geogr., 26, 165–181, 2001.
Myhre, G., Grini, A., Haywood, J. M., Stordal, F., Chatenet, B., Tanré, D., Sundet, J. K., and

ACPD
11, 7155–7187, 2011

Isaksen, I. S.: Modeling the radiative impact of mineral dust during the Saharan Dust Experiment (SHADE) campaign, J. Geophys. Res., 108, 8579, doi:10.1029/2002JD002566, 2003.
Redelsperger, J. L., Thorncroft, C. D., Diedhiou, A. Lebel, T., Parker, D. J., and Polcher, J.: African Monsoon Multidisciplinary Analysis: An International Research Project and Field Campaign, B. Am. Meteorol. Soc., 87, 1739–1746, 2006.
Saunois, M., Reeves, C. E., Mari, C. H., Murphy, J. G., Stewart, D. J., Mills, G. P., Oram, D. E., and Purvis, R. M.: Factors controlling the distribution of ozone in the West African lower troposphere during the AMMA (African Monsoon Multidisciplinary Analysis) wet season campaign, Atmos. Chem. Phys., 9, 6135–6155, doi:10.5194/acp-9-6135-2009, 2009.
Simpson, D., Guenther, A., Hewitt, C. N., and Steinbrecher, R.: Biogenic emissions in Europe. 1. Estimates and uncertainties, J. Geophys. Res., 100D, 22875–22890, 1995.
Stewart, D. J., Taylor, C. M., Reeves, C. E., and McQuaid, J. B.: Biogenic nitrogen oxide emissions from soils: impact on NO_x and ozone over west Africa during AMMA (African Monsoon Multidisciplinary Analysis): observational study, Atmos. Chem. Phys., 8, 2285–2297, doi:10.5194/acp-8-2285-2008, 2008.
Tang, Y., Carmichael, G. R., Kurata, G., Uno, I., Weber, R. J, Song, C-H., Guttikunda, S. K., Woo, J-H., Streets ,D. G., Wei, C., Clarke, A. D., Huebert, B., and Anderson, T. L.: Impacts of dust on regional tropospheric chemistry during the ACE-Asia experiment: A model study with observations, J. Geophys. Res., 109, D19S21, doi:10.1029/2003JD003806, 2004.
Twohy, C. H., Kreidenweis, S. M., Eidhammer, T., Browell, E. V., Heymsfield, A. J., Bansemer, A. R., Anderson, B. E., Chen, G., Ismail, S., Demott, P. J., and Van Den Heever, S. C.: Saharan dust particles nucleate droplets in eastern Atlantic clouds, Geophys. Res. Lett., 36, L01807, doi:10.1029/2008GL035846, 2009.
van der A, R. J., Eskes, H. J., Boersma, K. F., van Noije, T. P. C., Van Roozendael, M., De Smedt, I., Peters, D. H. M. U., and Meijer E. W.: Trends, seasonal variability and dominant NO_x source derived from a ten year record of NO_2 measured from space, J. Geophys. Res., 113, D04302, doi:10.1029/2007JD009021, 2008.
Vlasenko, A., Sjogren, S., Weingartner, E., Stemmler, K., Gäggeler, H. W., and Ammann, M.: Effect of humidity on nitric acid uptake to mineral dust aerosol particles, Atmos. Chem. Phys., 6, 2147–2160, doi:10.5194/acp-6-2147-2006, 2006.
Williams, J. E., Scheele, M. P., van Velthoven, P. F. J., Cammas, J.-P., Thouret, V., Galy-Lacaux, C., and Volz-Thomas, A.: The influence of biogenic emissions from Africa on tropical tropospheric ozone during 2006: a global modeling study, Atmos. Chem. Phys., 9, 5729–5749,

ACPD
11, 7155–7187, 2011

doi:10.5194/acp-9-5729-2009, 2009.
Zhang, Y., Sunwoo, Y., Kotamarthi, V., and Carmichael, G. R.: Photochemical Oxidant Processes in the Presence of Dust: An Evaluation of the Impact of Dust on Particulate Nitrate and Ozone Formation, J. Appl. Meteorol., 33,813–824, 1994.
Ziemke, J. R., Chandra, S., Duncan, B. N., Froidevaux, L., Bhartia, P. K., Levelt, P. F., and Waters, J. W.: Tropospheric ozone determined from Aura OMI and MLS: Evaluation of measurements and comparison with the Global Modeling Initiative's Chemical Transport Model, J. Geophys. Res., 111, D19303, doi:10.1029/2006JD007089, 2006.
Zipser, E. J., Twohy, C. H., Tsay, S.-C., Hsu, N. C., Heymsfield G. M., Thornhill K. L, Tanelli S., Ross R., Krishnamurti, T. N., Ji, Q., Jenkins, G., Ismail, S., Ferrare, R., Chen, G., Browell, E. V., Anderson ,B., Hood, R., Goodman, H. M., Heymsfield, A., Halverson, J., Dunion, J. P., Douglas, M., and Cifelli, R. J.: The Saharan Air Layer and the Fate of African Easterly Waves – NASA's AMMA Field Study of Tropical Cyclogenesis, B. Am. Meteorol. Soc., 90, 1137–1156, 2009.

ACPD
11, 7155–7187, 2011

Table 1. Surface −550 hPa Column O_3, Relative humidity and OMI AI index.

Date (2008)	Time (UTC)	O_3 925–550 hPa (DU)	RH 925–550 hPa(%)	OMI AI (13–16° N, 16–19° W)
8 June	1200	6.6	32.2	2.11
10 June	1200	7.4	37.3	1.29
12 June	1200	20.5	65.1	
15 June	1200	11.3	28.7	2.02
26 June	1200	10.5	37.2	1.98
2 July	1200	14.2	67.3	
2 August	1200	10.3	31.3	3.80
27 August	1200	6.4	88.5	0.58
3 September	1200	11.0	68.8	0.61

ACPD
11, 7155–7187, 2011

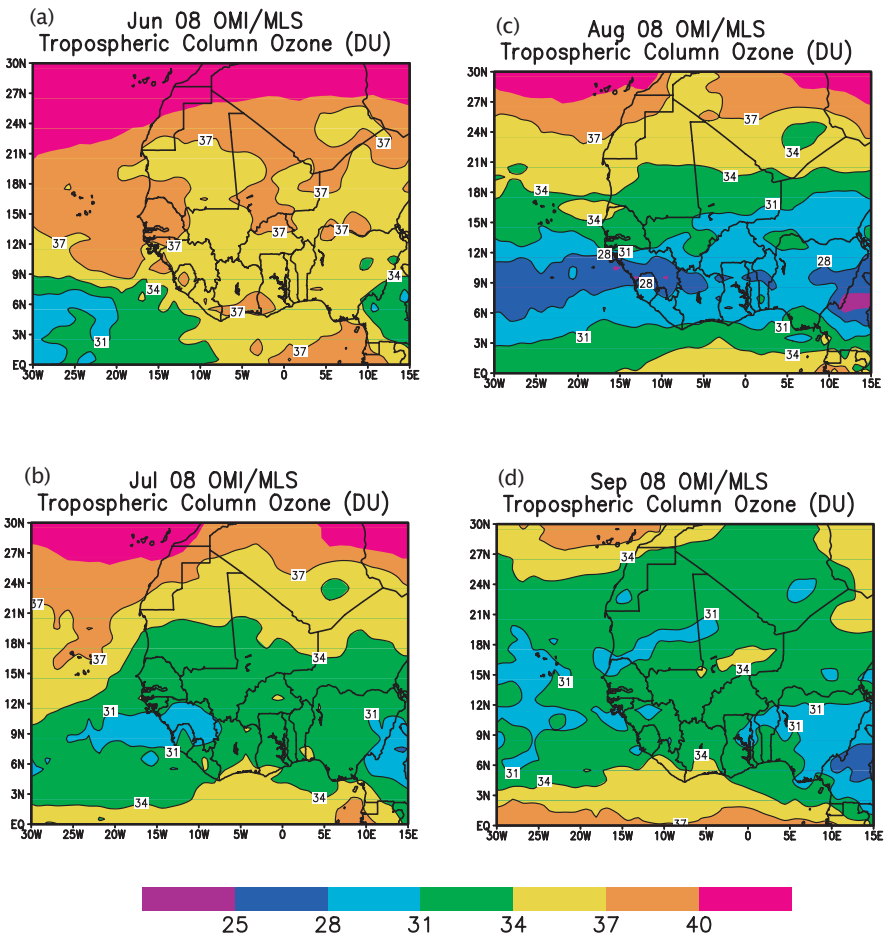

Fig. 1. OMI/MLS Total Column Ozone for **(a)** June 2008; **(b)** July 2008; **(c)** August 2008; **(d)** September 2008. Units are in DU.

ACPD
11, 7155–7187, 2011

Enhancement and depletion of tropospheric ozone in Senegal

G. S. Jenkins et al.

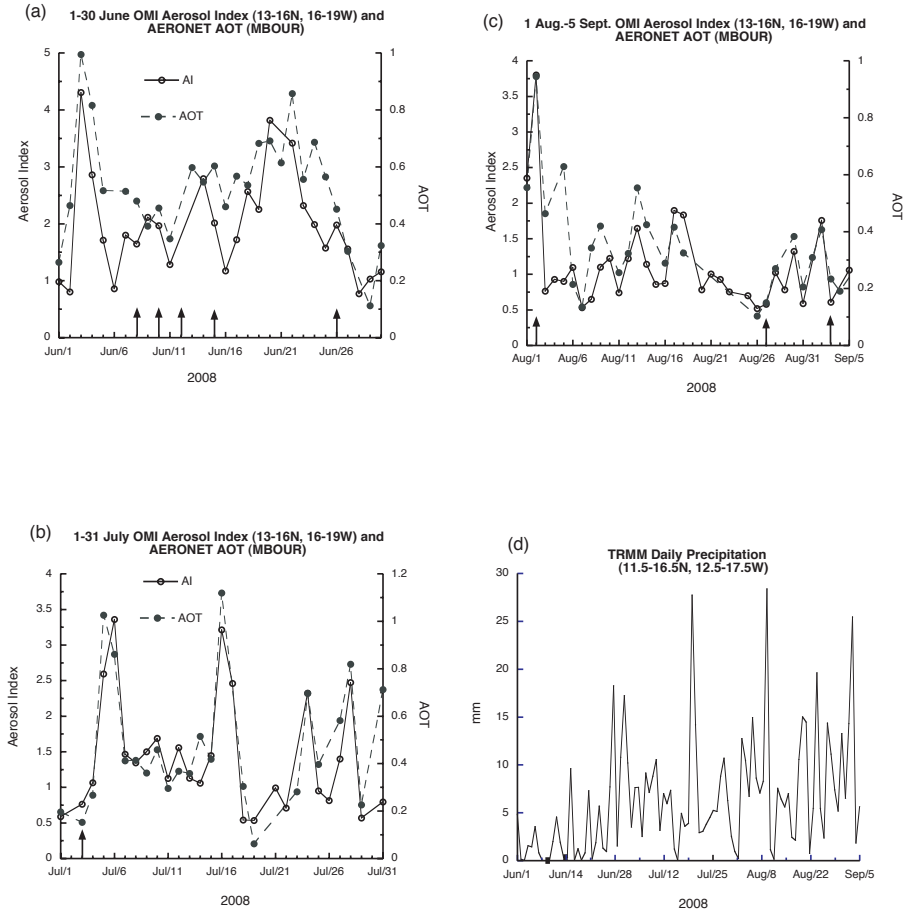

Fig. 2. Daily area averaged (13–16° N, 16–19° W) OMI derived Aerosol Index (AI) and Mbour, Senegal AOT for: **(a)** June; **(b)** July; **(c)** 1 August–5 September; **(d)** area averaged (11.5–16.5° N, 12.5–17.5° W) TRMM daily averaged precipitation for 1 June–5 September 2006.

ACPD
11, 7155–7187, 2011

Enhancement and depletion of tropospheric ozone in Senegal

G. S. Jenkins et al.

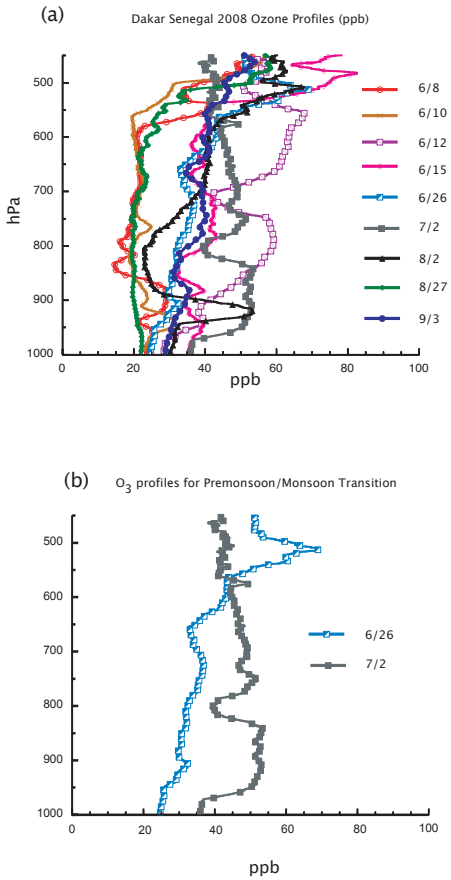

Fig. 3. 1000–450 hPa lower/middle tropospheric vertical profiles of O_3 concentrations for: **(a)** all launches; **(b)** 26 June and 2 July. Units are ppb.

ACPD
11, 7155–7187, 2011

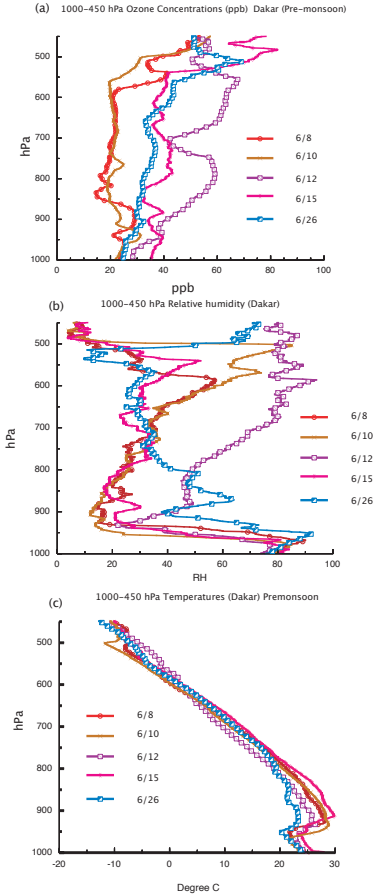

Fig. 4. 1000–450 hPa lower/middle tropospheric vertical profiles of: **(a)** O_3 concentrations; **(b)** relative humidity and **(c)** temperature for the pre-monsoon period.

ACPD
11, 7155–7187, 2011

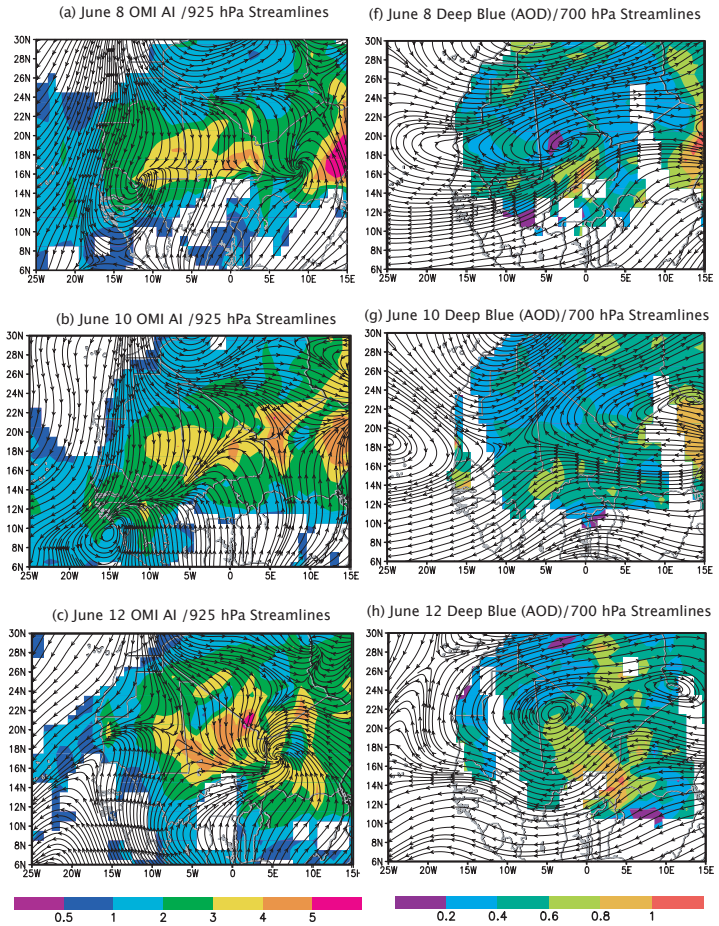

Fig. 5. re-Monsoon OMI AI/925 hPa streamlines and Deep Blue AOT/700 hPa streamlines: **(a, f)** 8 June; **(b, g)** 10 June; **(c, h)** 12 June; **(d, i)** 15 June; **(e, j)** 26 June.

ACPD
11, 7155–7187, 2011

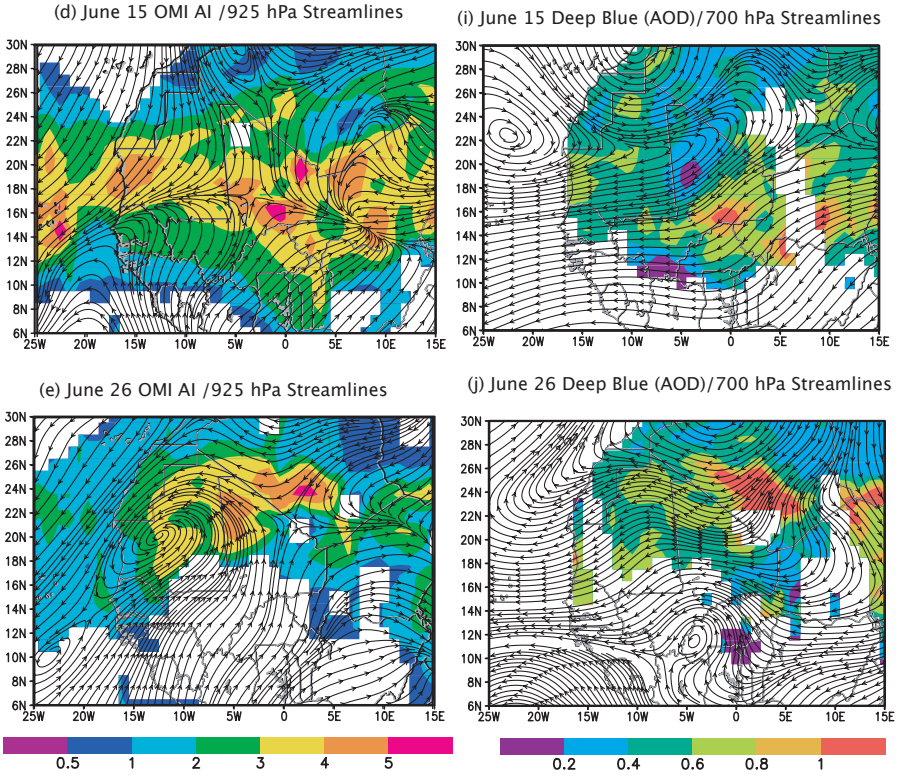

Fig. 5. Continued.

ACPD
11, 7155–7187, 2011

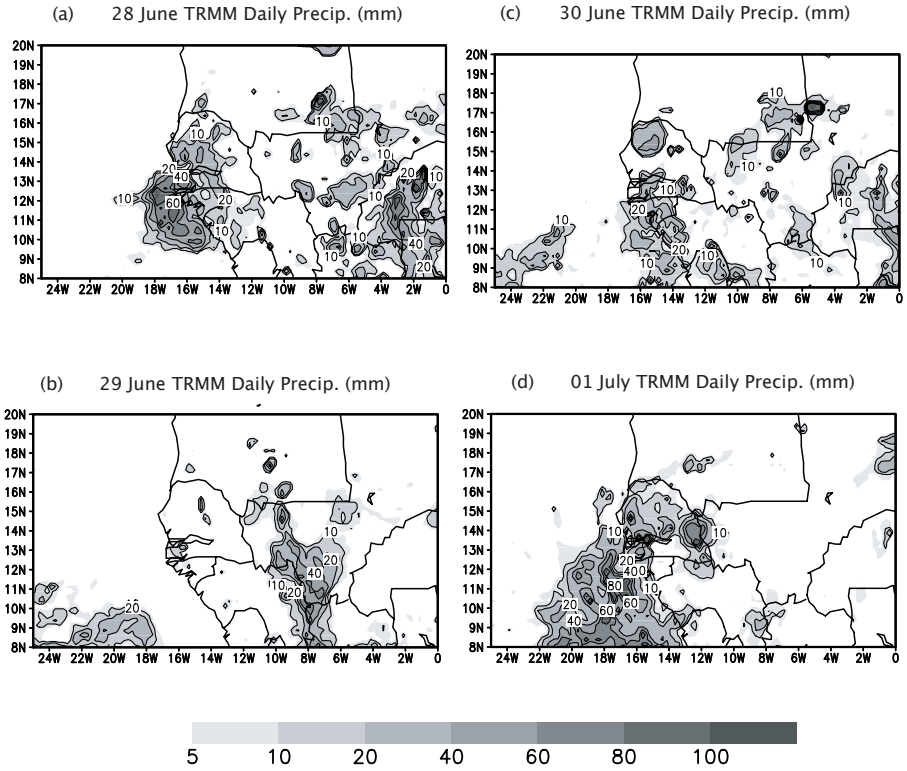

Fig. 6. TRMM daily Precipitation amounts **(a)** 28 June; **(b)** 29 June; **(c)** 30 June; **(d)** 1 July. Units are mm.

ACPD
11, 7155–7187, 2011

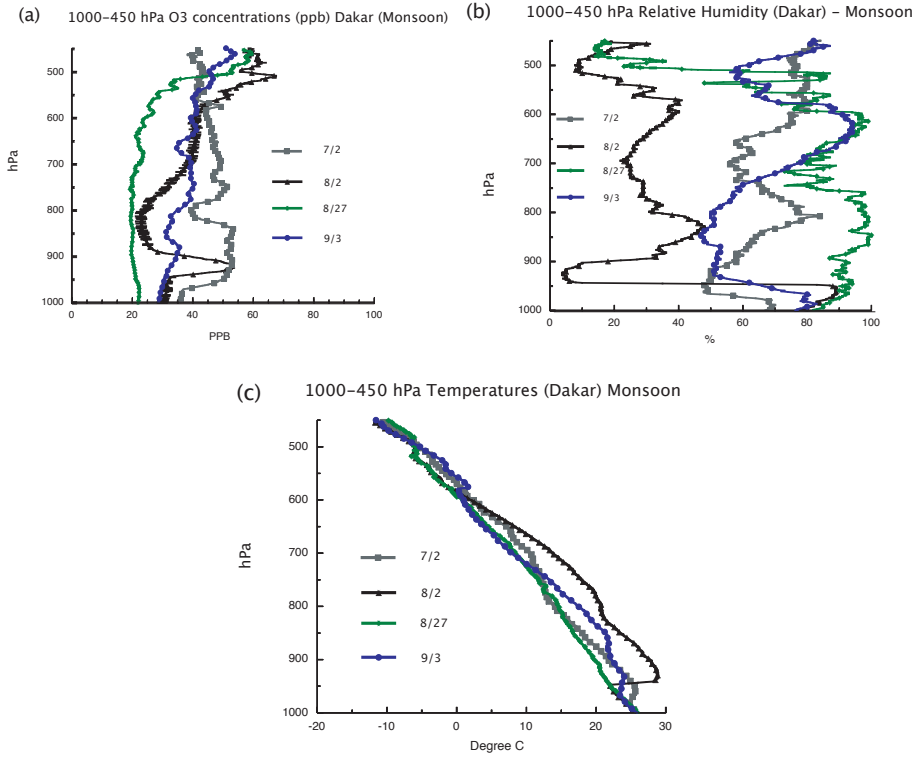

Fig. 7. 1000–450 hPa lower/middle tropospheric vertical profiles of: **(a)** O_3 concentrations; **(b)** relative humidity and **(c)** temperature for the monsoon period.

ACPD
11, 7155–7187, 2011

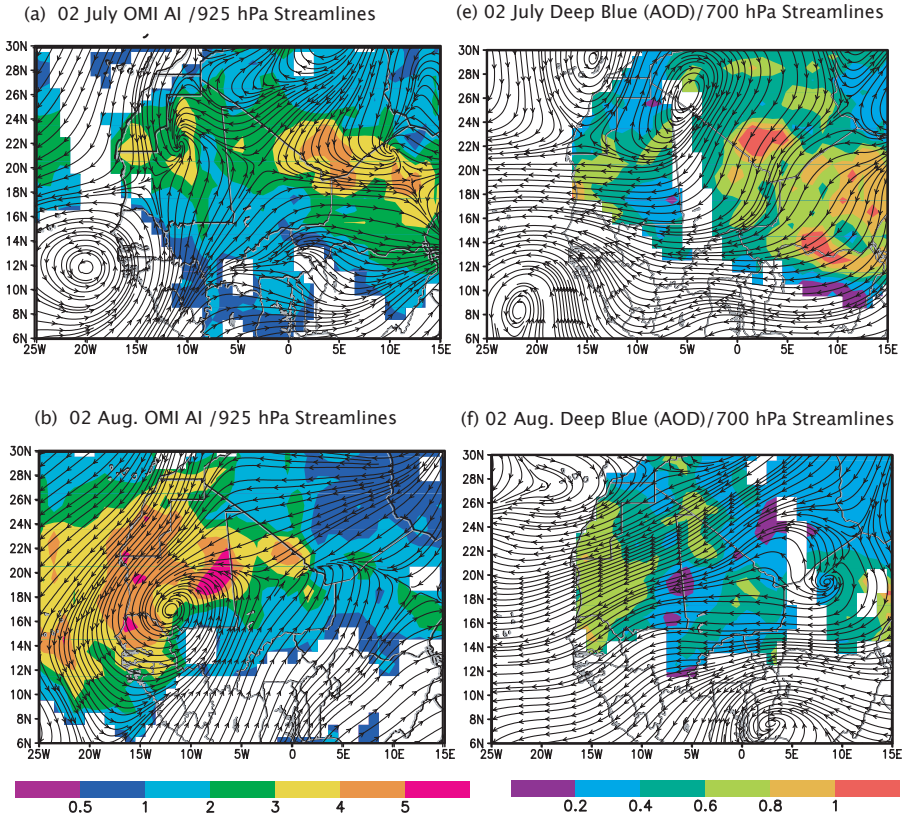

Fig. 8. Monsoon OMI AI/925 hPa streamlines and Deep Blue AOT/700 hPa streamlines: **(a, e)** 2 July; **(b, f)** 2 August; **(c, g)** 27 August; **(d, h)** 3 September.

ACPD
11, 7155–7187, 2011

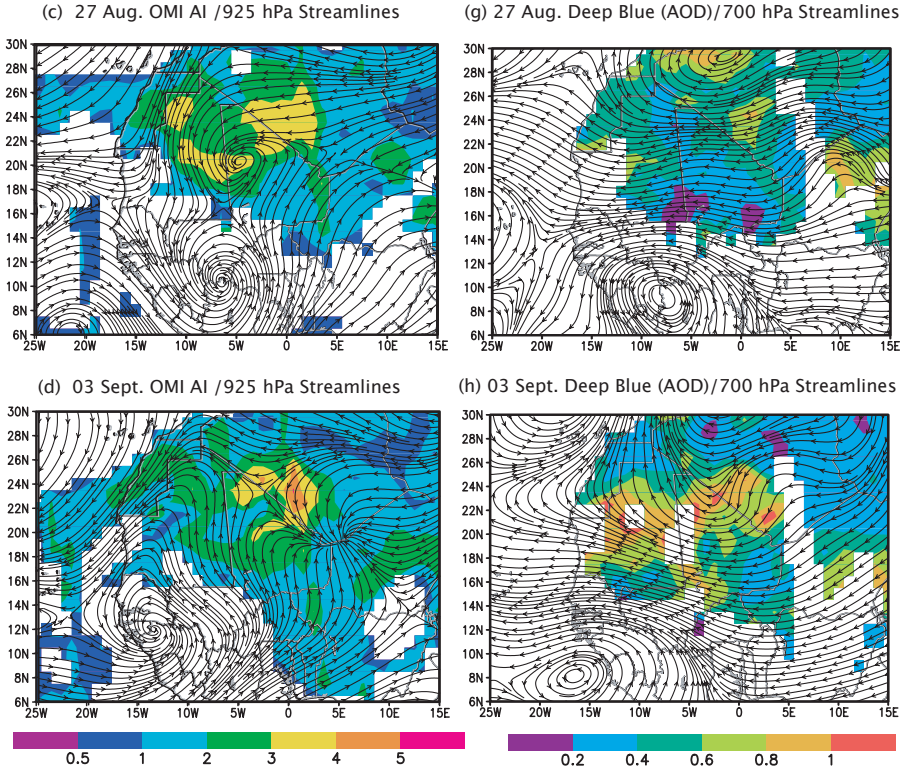

Fig. 8. Continued.

ACPD
11, 7155–7187, 2011

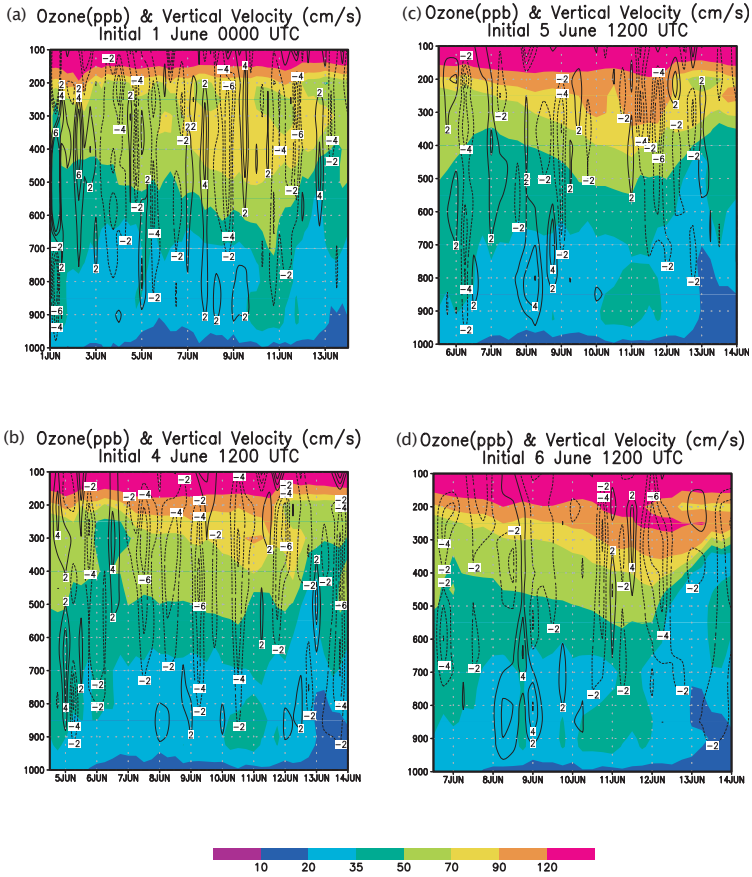

Fig. 9. Time-height profiles of O_3 concentrations and vertical velocity at 14.5° N, 17.5° W for initial conditions beginning at: **(a)** 1 June 00:00 UTC; **(b)** 4 June 12:00 UTC; **(c)** 5 June 12:00 UTC; **(d)** 6 June 12:00 UTC. Units in ppb and cm s^{-1}.

ACPD
11, 7155–7187, 2011

Enhancement and depletion of tropospheric ozone in Senegal

G. S. Jenkins et al.

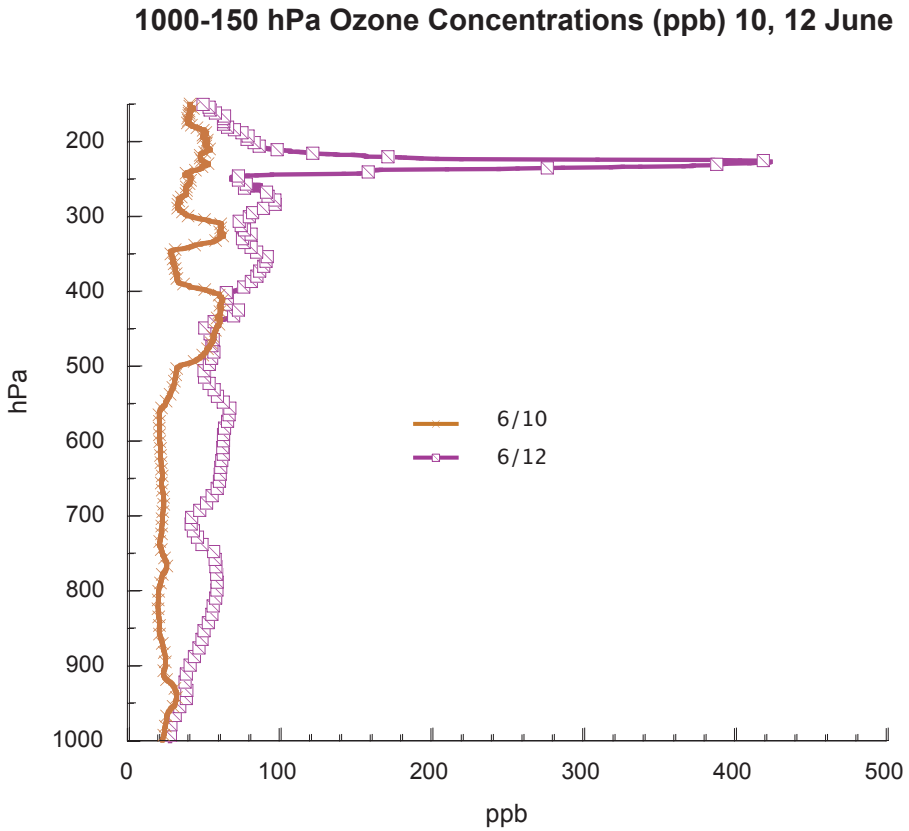

Fig. 10. 1000–150 hPa vertical profile of O_3 at Dakar for 10, 12 June, 12:00 UTC. Units in ppb.

ACPD
11, 7155–7187, 2011

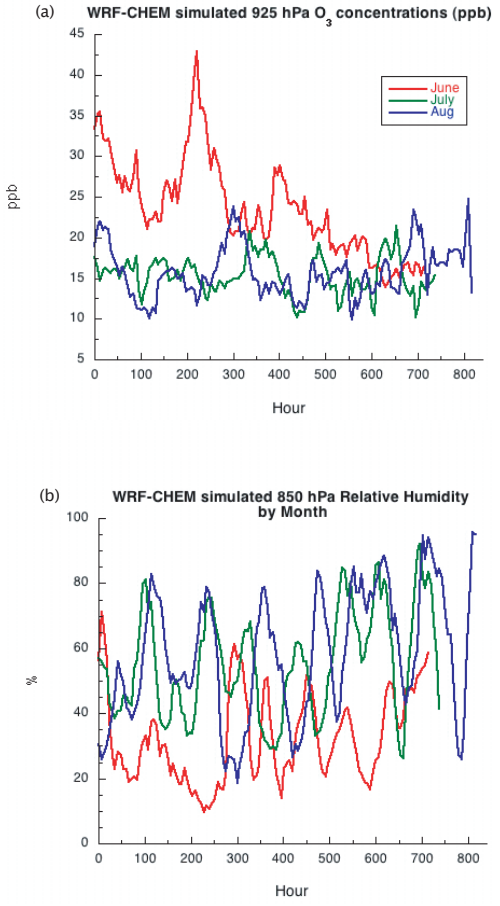

Fig. 11. WRF-Chem simulation of: **(a)** 925 hPa O_3 concentrations for June, July and August; **(b)** 850 hPa relative humidity for June, July and August.

ACPD
11, 7155–7187, 2011

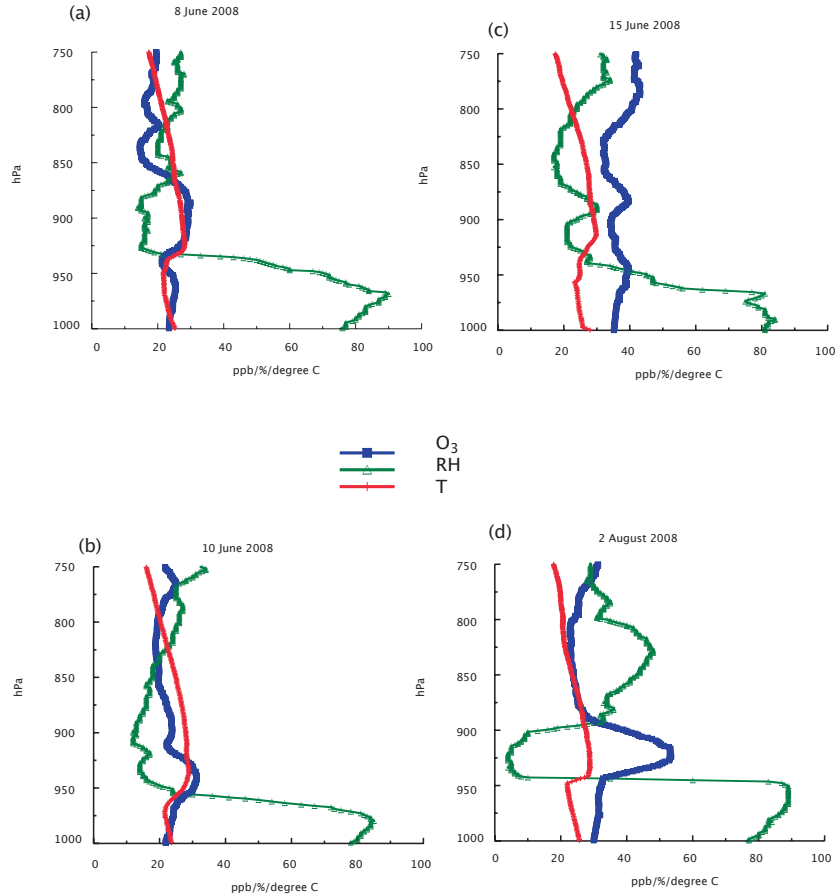

Fig. 12. 1000–750 hPa vertical profiles of O3 (blue), RH (green) and Temperature (red) for identified SAL events. **(a)** 8 June; **(b)** 10 June; **(c)** 15 June; **(d)** 2 August. Units are ppb for O_3, % for RH and Degree C for temperature.

ACPD
11, 7155–7187, 2011

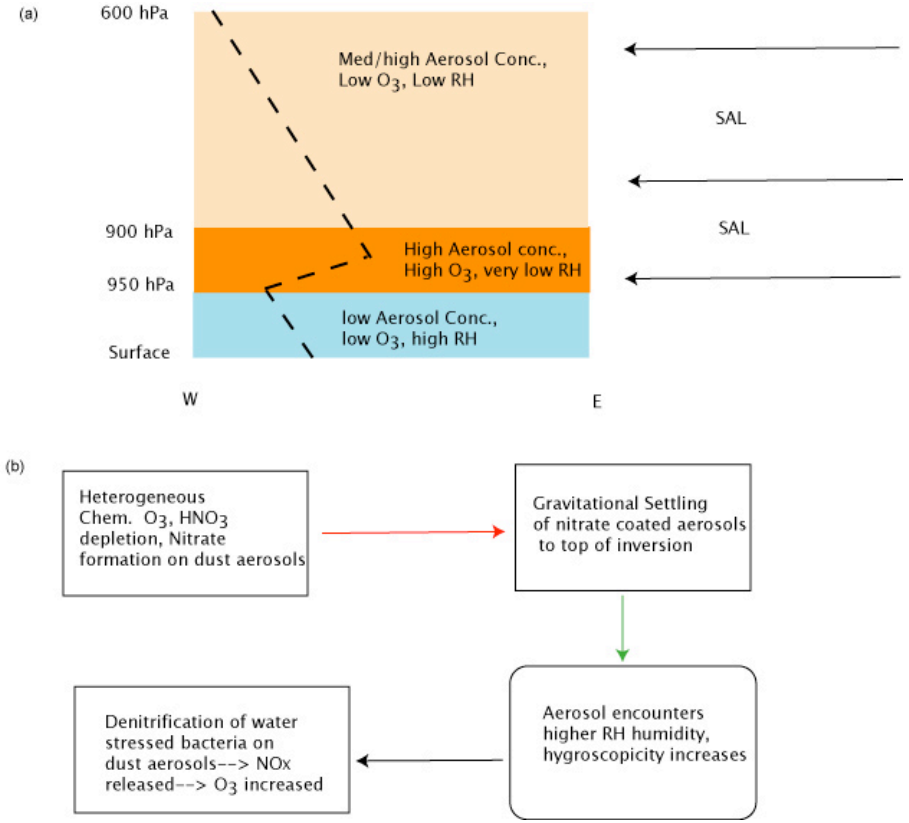

Fig. 13. **(a)** A depiction of relative humidity, aerosol and O_3 concentrations in various layer of the lower/middle troposphere associated with a SAL intrusion. The dash line represents the vertical profile of temperature. **(b)** Proposed mechanism for increasing O_3 in the 950–900 hPa layer.

ACPD
11, 7155–7187, 2011